Self-assembling optically-programmable apertures

Raphael Kay[a,b,c], Charlie Katrycz[a], Benjamin D. Hatton[a]

[a]Department of Materials Science and Engineering, University of Toronto
[b]Department of Mechanical and Industrial Engineering, University of Toronto
[c]John H. Daniels Faculty of Architecture, Landscape, and Design, University of Toronto

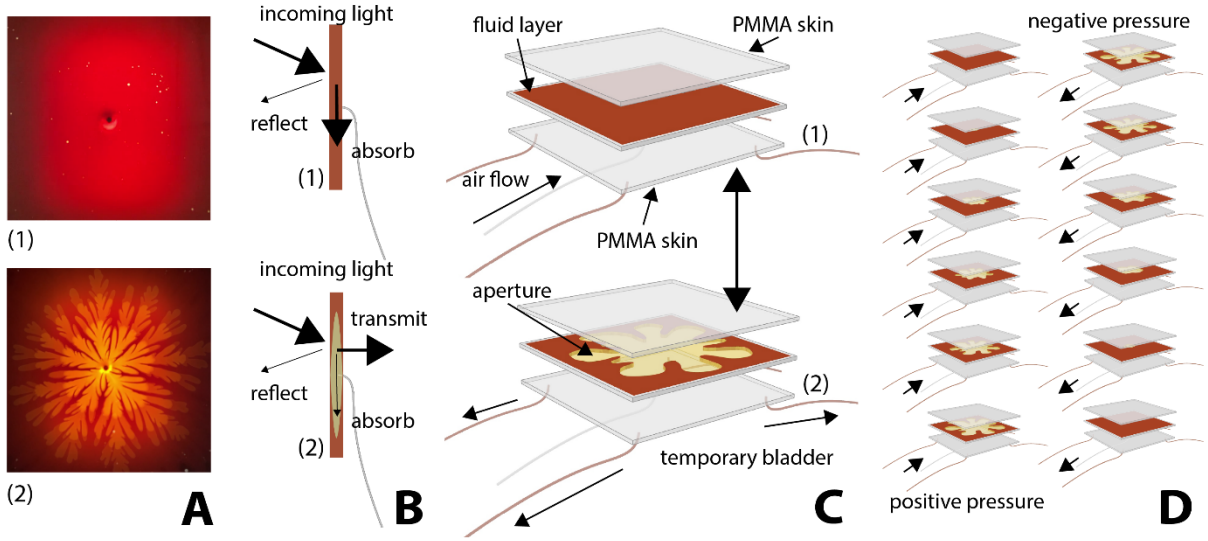

Figure 1. Design and reversible operation of shape-programmable aperture. (**A**) (1) Stable fluid layer prior to air injection. (2) Superimposed aperture opening sequence with positive air pressure. (**B**) Schematic showing ability of system to control light transmittance with aperture activation, where (1) represents closed state and (2) represents open state. (**C**) Design of fluidic device in which aperture is activated. (1) represents closed state and (2) represents open state. (**D**) From top-left to bottom-right, showing aperture opening and closing sequence, where positive pressure is applied for opening and negative pressure is applied for closing.

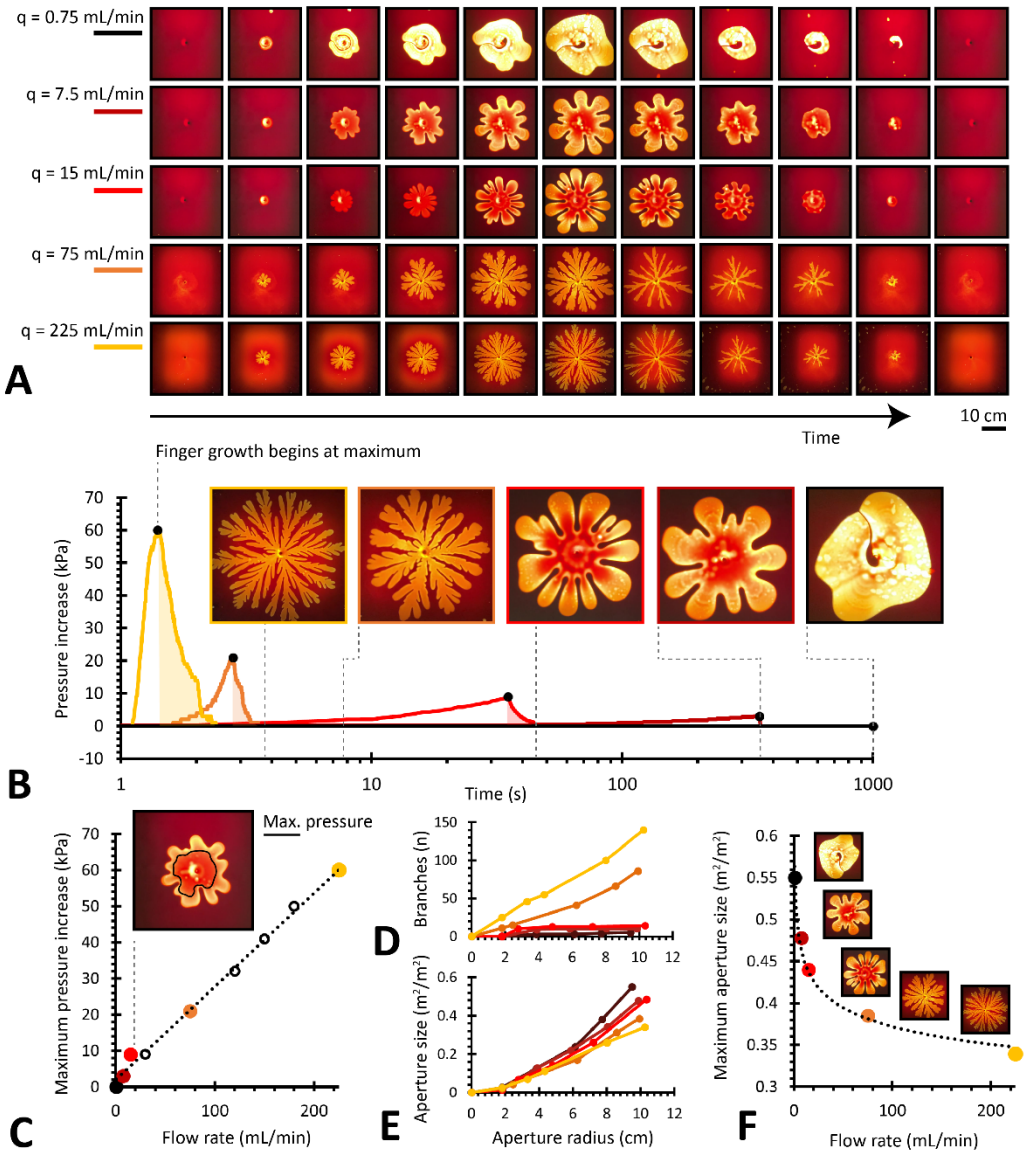

Figure 2. Aperture morphology can be programmed with flow rate. (**A**) Reversible aperture expansion and retraction sequence at five constant flow rates (0.75-225 mL/min). (**B**) Air pressure within aperture during expansion sequence. Maximum pressure occurs directly before branching begins, after which air pressure returns to P_{atm}. Images correspond to final morphology for each aperture. (**C**) Maximum air pressure increases linearly with flow rate. Maximum air pressure occurs at point in growth directly before branching begins, illustrated by black line in photo. (**D**) Number of branches increases as the apertures grows in radius, but to a greater degree for apertures assembled at higher flow rates. (**E**) Aperture area increases as the apertures grows in radius, but to a greater degree for apertures assembled at lower flow rates, due to less branched morphologies. (**F**) The maximum aperture size, within a cell with a fixed radius, can therefore be programmed with flow rate. Higher flow rates produce apertures with more branched morphologies, and less area coverage.

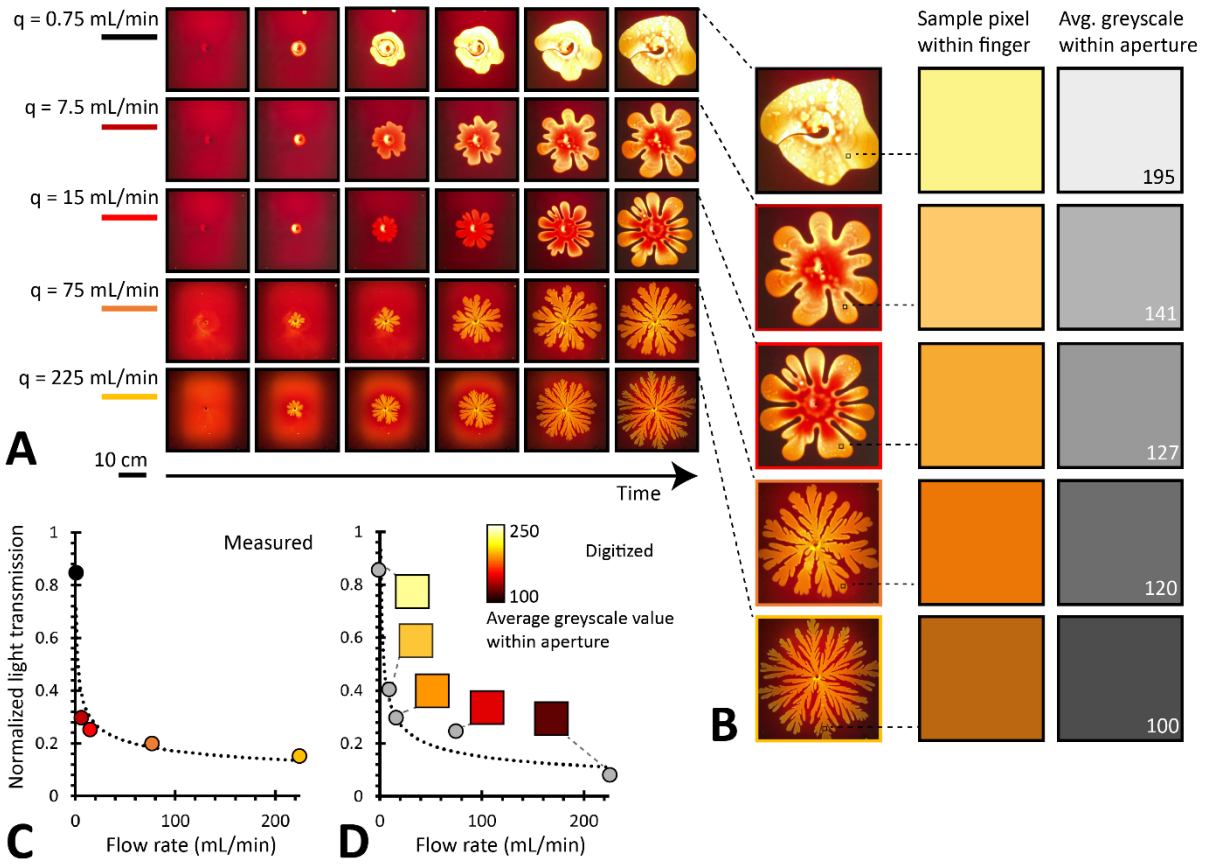

Figure 3. Aperture wetting and transmissivity can be programmed with flow rate. (**A**) Aperture expansion sequence at five constant flow rates (0.75-225 mL/min) within cell. (**B**) Pixel sampling from finger region of each aperture, indicative of differences in light transmissivity with consistent backlighting source. Average greyscale value (between 0-255) taken from aperture region, quantifying differences in transmissivity. (**C**) Average area-normalized light transmission intensity versus flow rate of injection. (**D**) Extrapolated light transmission intensity from digitized images and grey scale values from (B), remapped between measured light transmission values from (C). (C-D) represent two different methods of validating wetting trend, demonstrating variation in average film thickness within cell during aperture growth.

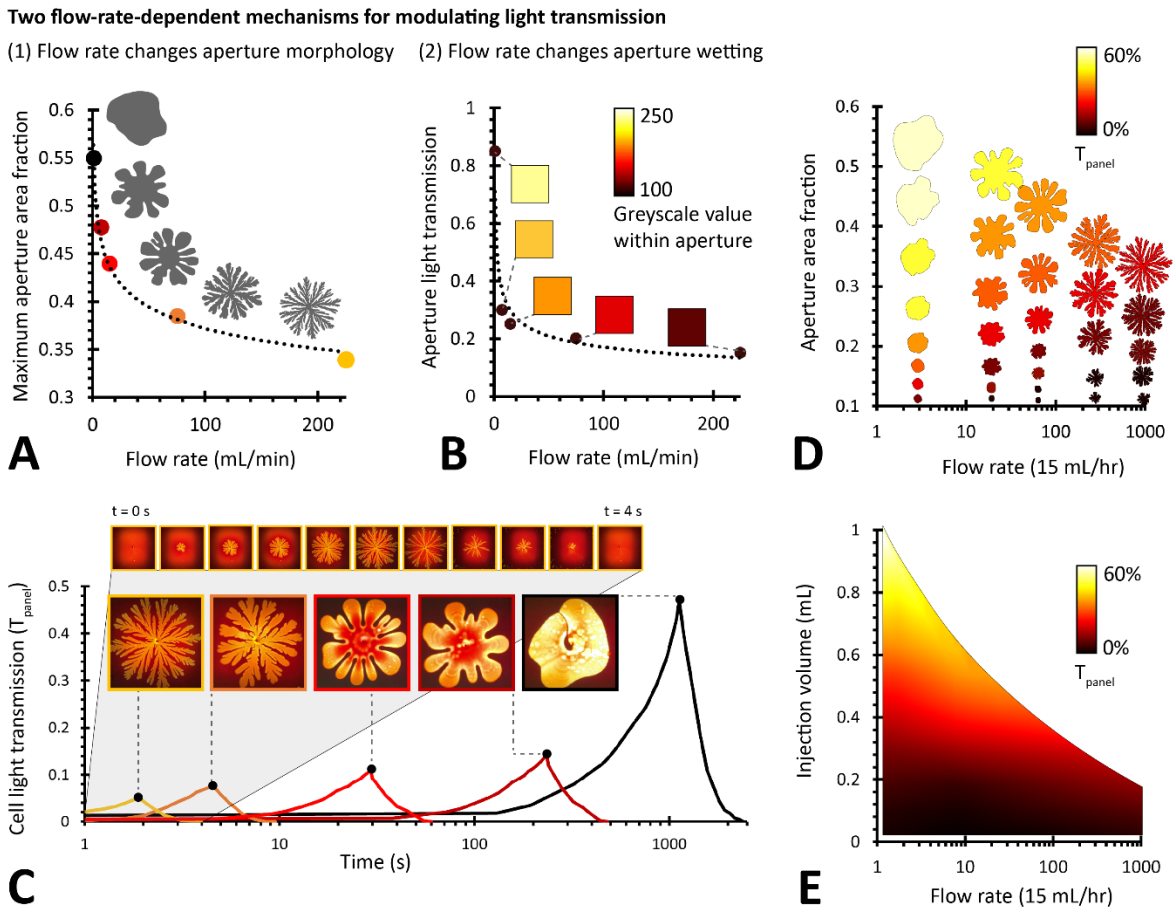

Figure 4. Cell transmissivity can be programmed with flow rate and injection volume. (**A-B**) Two mechanisms for modulating light transmission through a cell, each of which dependent on flow rate. (A) Aperture morphology and aperture area fraction can be programmed with flow rate. (B) Aperture wetting and light transmission intensity (area normalized) can be programmed with flow rate. Light transmission here is the measured light transmission through the aperture divided by the area of the aperture. This effect is confirmed by measuring average greyscale values within the aperture area, when backlit and photographed. Colour corresponds to average greyscale value, where higher values correspond to greater light transmission from the back light through the aperture. (**C**) Measured light transmission through the cell over time for five different aperture expansion and retraction sequences at five different flow rates (0.75-225 mL/min). (**D**) Functional range of aperture: Measured light transmission through the cell as a function of both aperture size (represented as a fraction of the cell) and flow rate. (**E**) Digital control space over aperture: Measured light transmission through the cell as a function of both air injection volume and air injection flow rate.

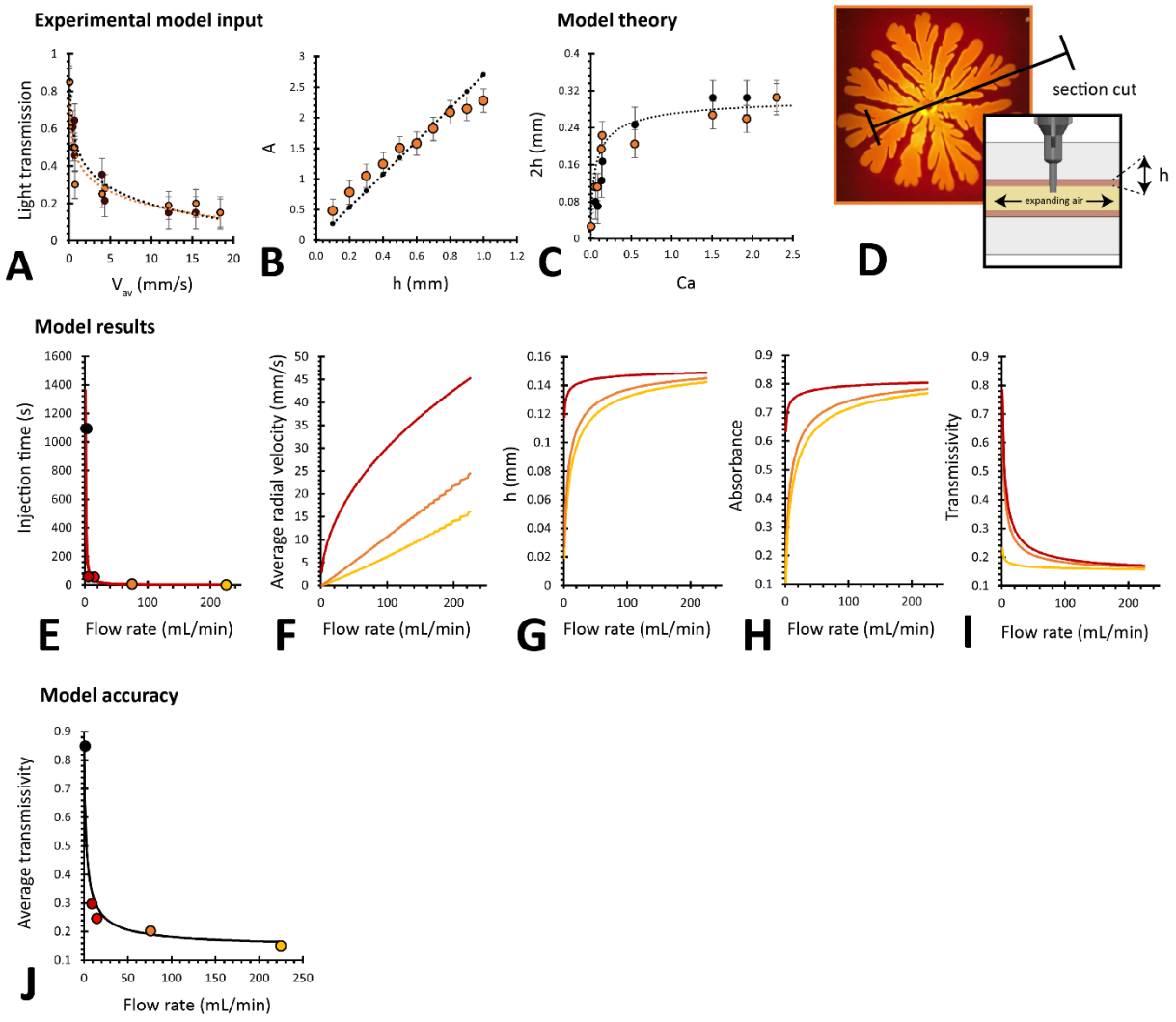

Figure 5. Mathematical model for measuring panel light transmission as function of flow rate. (**A**) Light transmission through aperture for different measured air velocities, where velocity changes thin film thickness (h) and total optical path length through cell (2h). Velocity values were measured over large areas, and were representative of the average. Black dots represent data extrapolated from grey-scale video frames. Orange dots represent directly measured light transmission data normalized by area. (**B**) Orange dots represent measured absorbance of molasses as function of optical path length (h), where absorbance, $A = -\log_{10} T$. Black dots represent absorbance values generated using Beer-Lambert model. Best fit of dotted black line provides absorption coefficient, ε, of 2.7 mm^{-1} for molasses. (**C**) Calculated thin film thickness versus Ca (Ca is directly proportional to velocity). Thickness values calculated using Beer-Lambert model with ε=2.7. Dotted black line represents fitted curve using the updated Bretherton model for the thickness of a wetting film as a function of Ca. Fitting parameters of ϕ=2.0 and τ=3.2 were used. (**D**) Cell schematic to show thin film thickness (h) within cell. (**E**) Modelled total injection time for aperture as a function of flow rate. Coloured dots represent true times from experiment. (**F**) Modelled average radial velocity as a function of flow rate. Burgundy, orange, and yellow curves represent maximum, minimum, and mean values calculated at each modelled flow rate. (**G**) Modelled thin film thickness as a function of flow rate. Burgundy, orange, and yellow curves

represent maximum, minimum, and mean values calculated at each modelled flow rate. (**H**) Modelled absorbance as a function of flow rate. Burgundy, orange, and yellow curves represent maximum, minimum, and mean values calculated at each modelled flow rate. (**I**) Modelled transmissivity as a function of flow rate. Burgundy, orange, and yellow curves represent maximum, minimum, and mean values calculated at each modelled flow rate. (**J**) Comparing modelled with measured average transmissivity as a function of flow rate. Model shows good accuracy for predicting average transmissivity.

Model

Consider an expanding 'two-dimensional' air bubble with a radius R_i that increases as a function of flow rate q, time t_i, and the depth of a cell it expands within $b - 2h$,

$$R_i = \sqrt{\frac{qt_i}{\pi(b-2h)}}$$

The maximum radius of the air bubble R_n depends on the total time of the air injection t_n, and determines when the model needs to be turned off,

$$R_n = \sqrt{\frac{qt_n}{\pi(b-2h)}}$$

The total time of the air injection t_n is a function of the square-shaped radius of the container within which it grows R_{cell} and the velocity of the air bubble V_{max} (how quickly it reaches the edge of its container). For the entire growth period,

$$t_i < \frac{R_{cell}}{V_{max}}$$

But once the following expression becomes true, then t_n has been reached,

$$t_i = \frac{R_{cell}}{V_{max}}$$

We therefore can rewrite the above as,

$$t_n = \frac{R_{cell}}{V_{max}}$$

We extrapolated from our physical experiments the maximum velocity of the air bubble V_{max} as a function of the flow rate of the air injection q,

$$V_{max} = \frac{R_{cell}}{0.0000003 \cdot q^{(-1.222)}}$$

This is not to be confused by the average velocity v_{i+1} between time t_i and time t_{i+1}, which is given by,

$$v_{i+1} = \frac{q}{\pi b} \cdot \frac{R_{i+1} - R_i}{{R_{i+1}}^2 - {R_i}^2}$$

The capillary number Ca_i is a function of the average velocity v_i,

$$Ca_i = \frac{v_i \Delta n}{\sigma}$$

The thickness of the leftover fluid h_i (not displaced by a moving air bubble) is a function of the capillary number Ca_i,

$$h_i = \frac{0.5b \cdot \varphi \cdot {Ca_i}^{2/3}}{1 + ([\varphi \cdot \omega] \cdot {Ca_i}^{\frac{2}{3}})}$$

Absorbance A_i is related to the thickness of the fluid film h_i that light must travel through,

$$A_i = 2h_i \cdot \varepsilon$$

Transmittance T_i is related to absorbance A_i,

$$T_i = 10^{[-1 \cdot A_i]}$$

The average transmittance across the fluid bubble $T_{avg}(q)$ is the average transmittance at every time stamp of the air bubble injection,

$$T_{avg}(q) = \frac{1}{n}\sum_{i=1}^{n} T_i$$

The area fraction $af_i(q)$ for the air bubble is proportional to the area of the bubble (numerator) divided by the area of the cell (denominator), where the area of the bubble is dependent on the radius of the air bubble R_i,

$$af_i(q) = \frac{\pi \cdot {R_i}^2}{2{R_{cell}}^2}$$

We can multiple the average transmittance across the fluid bubble $T_{avg}(q)$ by the maximum area fraction $af_n(q)$ for the air bubble to get the total maximum transmission through the panel $t_{panel}(q)$,

$$t_{panel}(q) = T_{avg}(q) \cdot af_n(q)$$